

## A fission model approach to alpha decay and cluster radioactivity of Dy, Er, and Yb isotopes

Kizhakkath Kalam GIRIJA,<sup>1,\*</sup> Antony JOSEPH<sup>2</sup>

<sup>1</sup>Department of Physics, University of Calicut, Kerala, India and Department of Physics,  
M.P.M.M.S.N.Trusts College, Shoranur, Kerala, India

<sup>2</sup>Department of Physics, University of Calicut, Kerala, India

Received: 10.07.2012 • Accepted: 09.10.2012 • Published Online: 19.06.2013 • Printed: 12.07.2013

**Abstract:** Rare earth nuclei are probable candidates for exhibiting cluster radioactivity. In the present work, a theoretical study of  $\alpha$  decay and heavy cluster emission from Dy, Er, and Yb nuclei in the mass range  $150 < A < 190$  has been carried out in a fission model approach. Some of the proton-rich isotopes of these nuclei are found to have long half-lives, but within the measurable range. Many of the neutron-rich isotopes under consideration are far from  $\beta$  stability and the most probable light clusters predicted are highly exotic in nature and the corresponding half-lives are extremely short. However, the decays of most probable heavy clusters predicted have half-lives in the measurable range. The calculations on neutron-rich isotopes indicate the emergence of new magic numbers for protons and neutrons. The centrifugal barrier effect on decay rate of some proton-rich Er isotopes is also investigated.

**Key words:**  $\alpha$  decay, probable cluster emissions, fission model, Q-value, half-life

### 1. Introduction

Cluster radioactivity has been a fascinating field for nuclear physicists since 1980, when Sandulescu et al. [1] predicted the possibility of clustering of nucleons into nuclei heavier than  $\alpha$  particles and their spontaneous emission without being accompanied by neutrons. Being a rare process, it took 4 years to observe the phenomenon after its prediction. In 1984, Rose and Jones [2] first observed cluster decay through the emission of  $^{14}\text{C}$  from  $^{223}\text{Ra}$  nucleus with  $^{209}\text{Pb}$  as daughter. Later, many other cluster emissions were reported [3]. All the actually observed clusters are neutron-rich, even-even, except  $^{23}\text{F}$  [4]. The heaviest cluster so far observed is  $^{34}\text{Si}$  [3],[5],[6].

Cluster radioactivity is commonly observed in the mass region  $A > 220$  [2] with the daughter around doubly magic  $^{208}\text{Pb}$ . The Quantum Mechanical Fragmentation Theory (QMFT) [7],[8] later predicted 2 more islands of cluster radioactivity around  $^{100}\text{Sn}$  [9] and  $^{132}\text{Sn}$  [10] daughters (Sn radioactivity). The heavy particle radioactivity from superheavy nuclei is theoretically developed by Poenaru et al. [11], [12]. It has been established that the cluster emission from odd parent nuclei is in many cases hindered as compared to those from the neighbouring even-even isotopes [13] and hence even isotopes are better cluster emitters than the odd mass ones. Moreover, the observed decays, where the parent and daughter nuclei have odd mass, are less in number [14]. In the present study, we have made an attempt to investigate the  $\alpha$  decay and cluster radioactivity

\*Correspondence: girijacus@gmail.com

from proton-rich and neutron-rich isotopes of the rare earth nuclei Dy, Er, and Yb in a fission model approach, which is more suitable for spherical nuclei.

The half-lives ( $T_{1/2}$ ) relevant to  $\alpha$  and cluster decays of all isotopes of these nuclei from  $A = 150$  to 190 are estimated using the fission model potential. In these calculations the instability against different cluster decays is studied, keeping the upper limit of half-life as  $10^{40}$  s, even though the actual limit of experimental measurement is far below this ( $10^{29}$  s). We got distinct regions of stability and instability in these 3 cases. The proton-rich and neutron-rich isotopes are found to have entirely different behavior with respect to the emission of probable clusters, shell closure property of the daughter nuclei, and Sn radioactivity. The minimum half-lives computed confirm the role of closed shell effects in cluster emission. It is also striking that the cluster radioactivity of proton-rich isotopes is in support of the existing magic numbers, but that of neutron-rich isotopes provides the possibility for the emergence of new magic numbers for protons and neutrons. The calculated half-lives of proton-rich Er isotopes show their dependence on orbital angular momentum due to the presence of centrifugal potential.

## 2. Theoretical formalisms

Cluster radioactivity is a very asymmetric fission mode that occurs only when the parent is in a metastable state. It can be explained either using the preformed cluster model (PCM) of Gupta and collaborators [15] or by the fission model of Poenaru et al. [16], on the basis of QMFT [7],[8]. In PCM, the preformation factor  $P_0$  is calculated explicitly. In the fission model approach, the nucleus undergoes continuous deformation as it penetrates through the nuclear potential barrier, until it attains the scission configuration. In fission model calculations, the shape parameterization is made by considering the decaying system as 2 spherical fragments in contact [17] as shown in Figure 1. The 4 independent coordinates selected [18] are the radii of spherical fragments  $R_1$  and  $R_2$ , the distance between their geometric centres  $\zeta$ , and the height of the largest segment  $\xi$ . At the end of evolution, the system approaches a limiting configuration of 2 spherical fragments of fixed radii  $\bar{R}_1$  and  $\bar{R}_2$ .

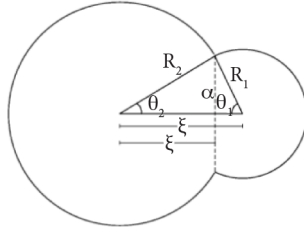


**Figure 1.** Schematic representation of shape parameterization of the decaying system in fission model approach [18].

In the present study, the 4-dimensional problem is reduced to a 1-dimensional one by imposing 3 constraints on the system. To preserve the adopted shape parameterization, the spheres should be in contact during the decay process, until the limiting configuration. For this, the geometrical constraint:

$$a^2 = R_1^2 - (\zeta - \xi)^2 \quad (1)$$

is imposed. Due to the incompressibility of nuclear matter, the conservation of total volume of the system is ensured by imposing the condition:

$$2(R_1^3 + R_2^3) + 3[R_1^2(\zeta - \xi) + R_2^2\xi] - [(\zeta - \xi)^3 + \xi^3] = 4R^3 \quad (2)$$

where  $R$  is the radius of the parent. The third constraint is associated with the flux of mass through the plane of intersection of the 2 spheroidal segments. For this, we assume a constant radius  $\bar{R}_1$  for the cluster throughout the evolution, i.e.

$$R_1 = \bar{R}_1 \quad (3)$$

Now, the 4-dimensional problem is reduced to a 1-dimensional one. The barrier penetrability factor  $P$  is estimated using the 1-dimensional WKB approximation [16] as:

$$P = \exp(-2/\hbar \int_{\zeta_1}^{\zeta_2} [2\mu(V - Q)]^{1/2} d\zeta) \quad (4)$$

with  $Q$  being the Q-value of the decay (energy released), which includes shell effects. Q-value is calculated in terms of mass excesses taken from the Nuclear Mass Data Table [19].  $\zeta_1$  and  $\zeta_2$  are the inner and outer turning points, respectively, which are given by [18]:

$$\zeta_1 = R - \bar{R}_1 \quad (5)$$

and

$$\zeta_2 = Z_1 Z_2 e^2 / Q \quad (6)$$

It is to be mentioned here that the deformations of parent and fragments modify the potential barrier and affect the decay rate. In this model, the deformation is not taken into account explicitly, but its effect is partially included through the Q-values used in the calculations [20],[21]. The radius of the parent  $R$  is determined by:

$$R = r_0 A^{1/3} \quad (7)$$

Here, the nuclear radius parameter  $r_0$  is adjusted to reproduce the available experimental data of  $\alpha$  decay and cluster emission and the most suited value is found to be 1.37 [17], [18],[22], [23]. The interacting potential  $V$  is the effective liquid drop one [22], which is the sum of Coulomb  $V_c$  and surface  $V_s$  potentials plus the centrifugal part  $V_l$ . The expression for  $V_c$  developed by Gaudin [24] is given as:

$$V_c = (8/9)\pi a^5 \epsilon(x_1, x_2) \rho_c \quad (8)$$

where  $\epsilon(x_1, x_2)$  is a function of angular variables:

$$x_1 = \pi - \theta_1 \quad (9)$$

and

$$x_2 = \theta_2 - \pi \quad (10)$$

Also  $\rho_c$  is the charge density and  $a$  is the radius of the neck. The surface potential is

$$V_s = 4\pi(R^2 - R_1^2 - R_2^2)\sigma_{eff} \quad (11)$$

where  $\sigma_{eff}$  is the effective surface tension. The centrifugal potential is

$$V_l = (\hbar^2/2\mu)l(l+1)/\zeta^2 \quad (12)$$

In the fission model, it is assumed that the system penetrates through the potential barrier  $V-Q$ . Here the shell effects reduce the Q value and hence enhance the height of the barrier  $V-Q$ , which causes a decrease in

penetrability and a longer half-life. To determine the inertia coefficient  $\mu$ , the Werner–Wheeler approximation [22] is made use of. To be consistent with the uniform charge distribution considered in the Coulomb potential, the final radii of fragments should be [18]:

$$\bar{R}_i = [Z_i/Z]^{1/3}R, \quad i = 1, 2. \quad (13)$$

The decay rate is

$$\lambda = \nu P \quad (14)$$

with the assault frequency  $\nu = 10^{22} s^{-1}$  [17],[18]. The half-life is calculated as:

$$T_{1/2} = \frac{0.693}{\lambda} \quad (15)$$

### 3. Results and discussion

Table 1 gives the mass regions of the nuclei studied, nuclei instable against  $\alpha$  emission and cluster decay, and nuclei stable against them. It is seen that there are alternate mass regions of stability and instability in the case of Dy, Er, and Yb nuclei. We have considered all possible combinations of parent and cluster for which the Q-value is positive and found that the probable decay modes in proton-rich isotopes are  $\alpha$ ,  ${}^8_4Be$ ,  ${}^{12}_6C$ , and  ${}^{16}_8O$  emissions, due to the lowest half-lives. Although some of the calculated half-lives are above the experimentally measurable limit, such high values are reported by Gupta et al. also in [25].

**Table 1.** Mass regions of stability and instability against  $\alpha$  and various cluster emissions in Dy, Er, and Yb isotopes.

Nucleus	${}_{66}Dy$	${}_{68}Er$	${}_{70}Yb$
Mass range studied	A: 150-190	A: 150-190	A: 150-190
Instable to $\alpha$ decay	A: 150-156	A: 150-163	A: 150-170
Instable to ${}^8Be$ decay	A: 152-153	A: 153-156	A: 155-159
Instable to ${}^{12}C$ decay	A: 152-155	A: 152-159	A: 150-162
Instable to ${}^{16}O$ decay	A: 155-156	A: 153, 155-159	A: 150-163
Stable	A: 157-173	A: 164-177	A: 171-181
Instable to exotic cluster decays	A: 174-181	A: 178-186	A: 182-190
Stable	A: 182-190	A: 187-190	-

Table 2 exhibits the calculated half-lives of proton rich Dy, Er, and Yb isotopes (for which experimental values are available) for  $\alpha$  decay and those of some actinide nuclei for cluster emission. The experimental values from [18] are shown in column 4. The observed agreement reiterates the suitability of the fission model approach for heavy cluster decay also. Figure 2 shows the variation in  $Log_{10}T_{1/2}$  of proton rich Dy, Er, and Yb isotopes with respect to the mass number of parents.

The minimum half-lives of proton-rich Dy, Er, and Yb isotopes for the prominent decay modes are shown in Table 3. The corresponding parent nuclei are given in brackets. It is found that in all these decays, the daughter is with a neutron number equal to or around an existing magic number (81 or 82) and the proton number is in the neighborhood of midway between magic numbers, which reveals the role of shell structure in cluster radioactivity. Figure 3 comprises the plots of calculated half-lives and Q-values (from mass tables [26]) for  $\alpha$  emission and various cluster decays of proton-rich Er isotopes against neutron number of daughter, which

**Table 2.** Calculated values of  $\text{Log}_{10}T_{1/2}$  of proton-rich Dy, Er, and Yb isotopes for  $\alpha$  decay and calculated values of  $\text{Log}_{10}T_{1/2}$  of some actinide nuclei for heavy cluster emissions. The experimental values (from Ref [18]) are also shown.

Parent	Mode of decay	$\text{Log}_{10}T_{1/2}$ ( $T_{1/2}$ in seconds)	
		Calculated	Experimental
$Dy^{150}$	$\alpha$	3.16	3.08
$Dy^{151}$	$\alpha$	4.17	4.28
$Dy^{152}$	$\alpha$	7.20	6.93
$Dy^{153}$	$\alpha$	8.46	8.38
$Dy^{154}$	$\alpha$	14.03	13.98
$Er^{152}$	$\alpha$	1.13	1.04
$Er^{153}$	$\alpha$	1.77	1.85
$Er^{154}$	$\alpha$	4.69	4.68
$Er^{155}$	$\alpha$	5.69	6.20
$Er^{156}$	$\alpha$	10.71	10.36
$Yb^{154}$	$\alpha$	-0.36	-0.36
$Yb^{155}$	$\alpha$	0.23	0.30
$Yb^{156}$	$\alpha$	2.77	2.41
$Yb^{157}$	$\alpha$	3.78	3.89
$Yb^{158}$	$\alpha$	6.52	6.66
$Fr^{221}$	$^{14}C$	14.42	14.46
$Ra^{221}$	$^{14}C$	13.26	13.41
$Ra^{226}$	$^{14}C$	21.84	21.30
$Ac^{225}$	$^{14}C$	17.86	17.15
$Th^{230}$	$^{24}Ne$	24.78	24.64
$U^{234}$	$^{24}Ne$	25.66	25.07
$Pu^{238}$	$^{28}Mg$	25.18	25.70

**Table 3.** Minimum values of  $\text{Log}_{10}T_{1/2}$  of proton-rich Dy, Er, and Yb nuclei for  $\alpha$  and various cluster emissions. Corresponding parent nuclei are given in brackets.

Nucleus	Minimum $\text{Log}_{10}T_{1/2}$ ( $T_{1/2}$ in seconds) for			
	$\alpha$ decay	$^8Be$ decay	$^{12}C$ decay	$^{16}O$ decay
Dy	3.1618 ( $^{150}Dy$ )	37.1684 ( $^{152}Dy$ )	32.7048 ( $^{154}Dy$ )	39.2361 ( $^{155}Dy$ )
Er	1.1304 ( $^{152}Er$ )	28.4844 ( $^{154}Er$ )	27.4947 ( $^{156}Er$ )	33.2822 ( $^{157}Er$ )
Yb	-0.3584 ( $^{154}Yb$ )	24.5929 ( $^{156}Yb$ )	22.6320 ( $^{158}Yb$ )	28.3304 ( $^{160}Yb$ )

are mirror reflections. These plots again confirm the shell closure at  $N = 82$  (only in the case of  $^{16}O$  decay, the minimum is at  $N = 81$ , but very near to  $N = 82$ ).

The effect of the centrifugal part of potential on half-life is studied in the case of proton-rich Er isotopes having minimum  $T_{1/2}$  against various cluster decays and is illustrated in Table 4. Figure 4 indicates the variation in logarithmic  $T_{1/2}$  with respect to  $l$  value. It is found that with the inclusion of centrifugal potential,  $T_{1/2}$  increases or the decay is slowed down and the change is appreciable only for high  $l$  values. It is also noted that the change in half-life is very significant for light clusters. The centrifugal barrier effect on the life time of  $^{151}Lu$ ,  $^{212}Po$ ,  $^{216}Rn$ ,  $^{222}Ra$ , and  $^{256}No$  for various charged particle emissions up to  $l = 15$  is studied by Poenaru et al. [16]. Our results are very similar to this.

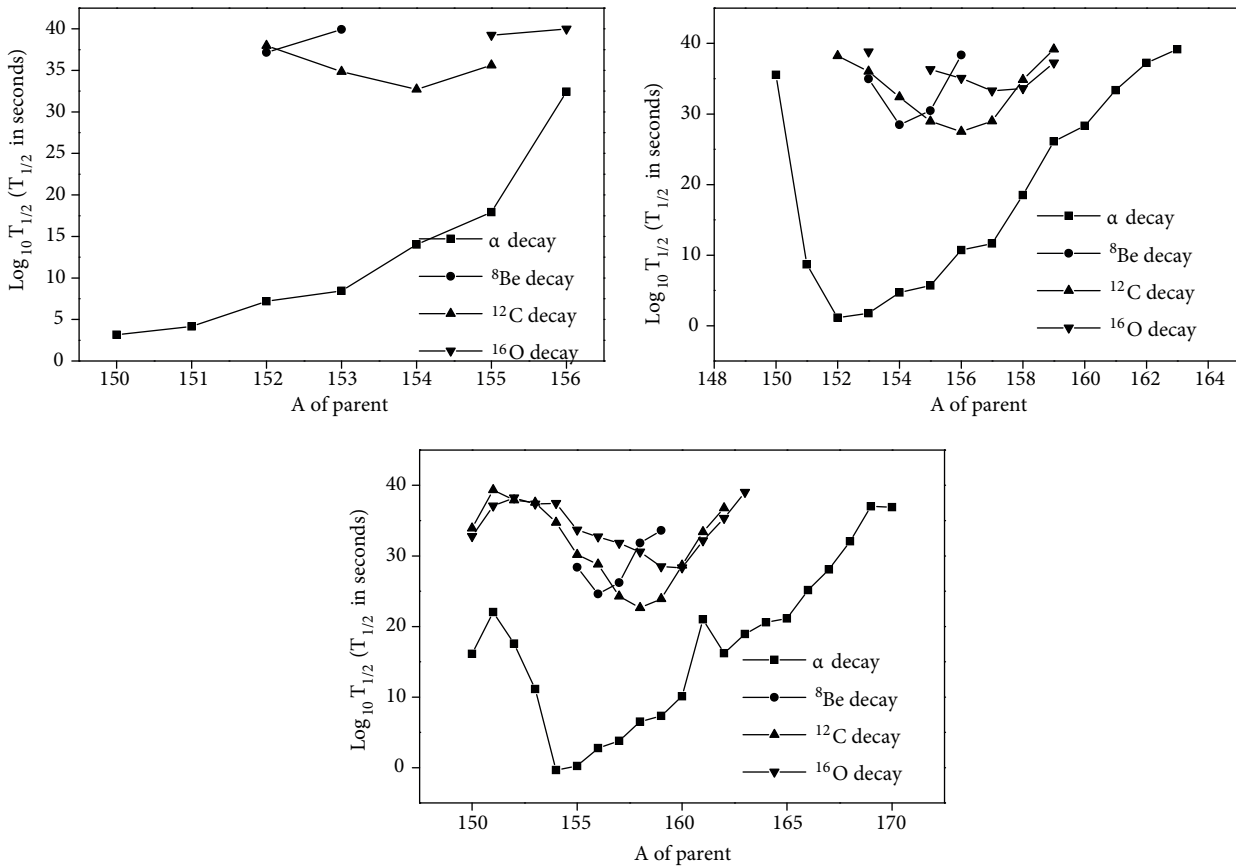


**Figure 2.** Plots of  $\text{Log}_{10} T_{1/2}$  of proton-rich Dy (top left), Er (top right), and Yb (bottom) isotopes against mass number of parents for different cluster decays.

The Geiger–Nuttall plots of the proton-rich Dy, Er, and Yb nuclei for  $\alpha$  decay and various cluster emissions are shown in Figure 5. The  $Q$ -values are computed on the basis of mass tables proposed by Audi et al. [26]. The slopes and  $Y$  intercepts of these plots take the general form:

$$\log T_{1/2} = \frac{X(Z_1)}{\sqrt{Q}} + Y(Z_1) \quad (16)$$

where  $Z_1$  is the proton number of cluster. The values  $X(Z_1)$  and  $Y(Z_1)$  are obtained as:

For Dy:

$$X(Z_1) = -64.1648Z_1^3 + 938.8452Z_1^2 - 1050.6972Z_1 + 2227.4236 \quad (17)$$

$$Y(Z_1) = 0.3992Z_1^3 - 4.9948Z_1^2 + 7.5719Z_1 - 46.3194 \quad (18)$$

For Er:

$$X(Z_1) = 22.9364Z_1^3 - 154.5791Z_1^2 + 3205.5975Z_1 - 2504.8460 \quad (19)$$

$$Y(Z_1) = -0.2300Z_1^3 + 3.0883Z_1^2 - 24.0491Z_1 - 10.7896 \quad (20)$$

and for Yb:

$$X(Z_1) = -31.8784Z_1^3 + 690.3105Z_1^2 - 760.0007Z_1 + 2581.0538 \quad (21)$$

Table 4.  $\text{Log}_{10}T_{1/2}$  of Er isotopes for different  $l$  values.

$l$	$\text{Log}_{10}T_{1/2}(T_{1/2}$ in seconds)			
	$\alpha$ decay of $^{152}\text{Er}$	$^8\text{Be}$ decay of $^{154}\text{Er}$	$^{12}\text{C}$ decay of $^{156}\text{Er}$	$^{16}\text{O}$ decay of $^{158}\text{Er}$
0	1.1304	28.4844	27.4947	33.6185
1	1.2126	28.5259	27.5206	33.6375
2	1.3764	28.6089	27.5722	33.6753
3	1.6211	28.7331	27.6497	33.7321
4	1.9451	28.8985	27.7529	33.8078
5	2.3467	29.1049	27.8817	33.9023
6	2.8240	29.3518	28.0361	34.0156
7	3.3746	29.6390	28.2160	34.1477
8	3.9960	29.9661	28.4212	34.2985
9	4.6857	30.3327	28.6516	34.4680
10	5.4411	30.7382	28.9070	34.6560
11	6.2595	31.1822	29.1872	34.8625
12	7.1383	31.6642	29.4921	35.0875

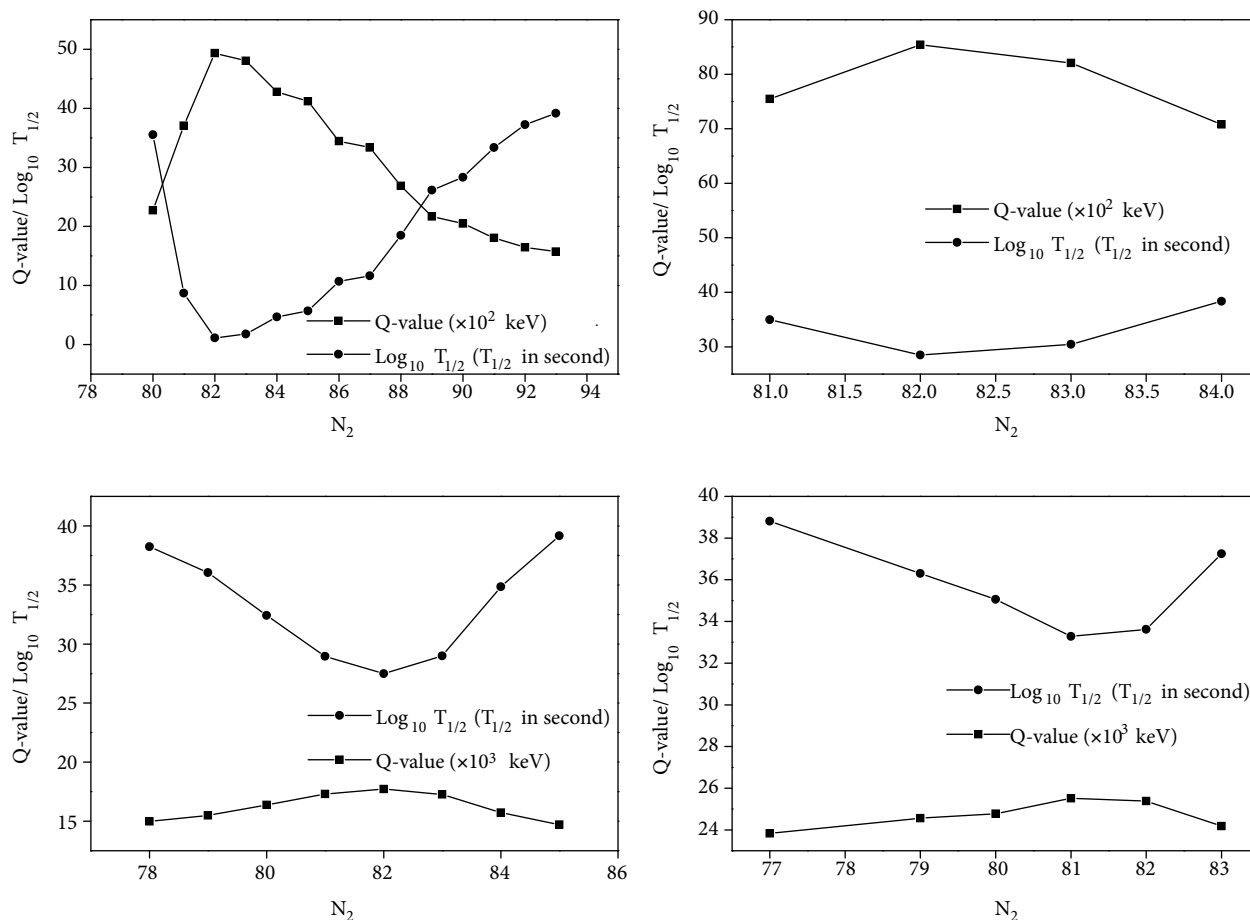
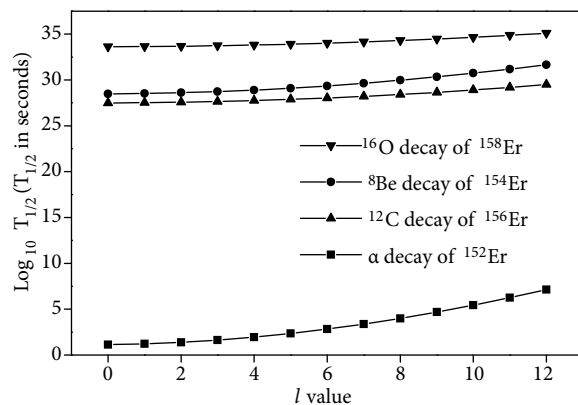


Figure 3. Plots of  $\text{Log}_{10}T_{1/2}$  and Q-values against neutron number of daughter nuclei, for  $\alpha$  decay (top left),  $^8\text{Be}$  decay (top right),  $^{12}\text{C}$  decay (bottom left), and  $^{16}\text{O}$  decay (bottom right) of Er isotopes.



**Figure 4.** Plots of  $\text{Log}_{10}T_{1/2}$  of Er isotopes for different cluster decays as function of  $l$  values.

$$Y(Z_1) = 0.3071Z_1^3 - 5.3836Z_1^2 + 16.8788Z_1 - 63.3258 \quad (22)$$

Recently, universal curves for  $\alpha$  emitters were prepared by Poenaru et al. [27] and a universal law that can describe all decay modes was developed by Qi et al. [28].

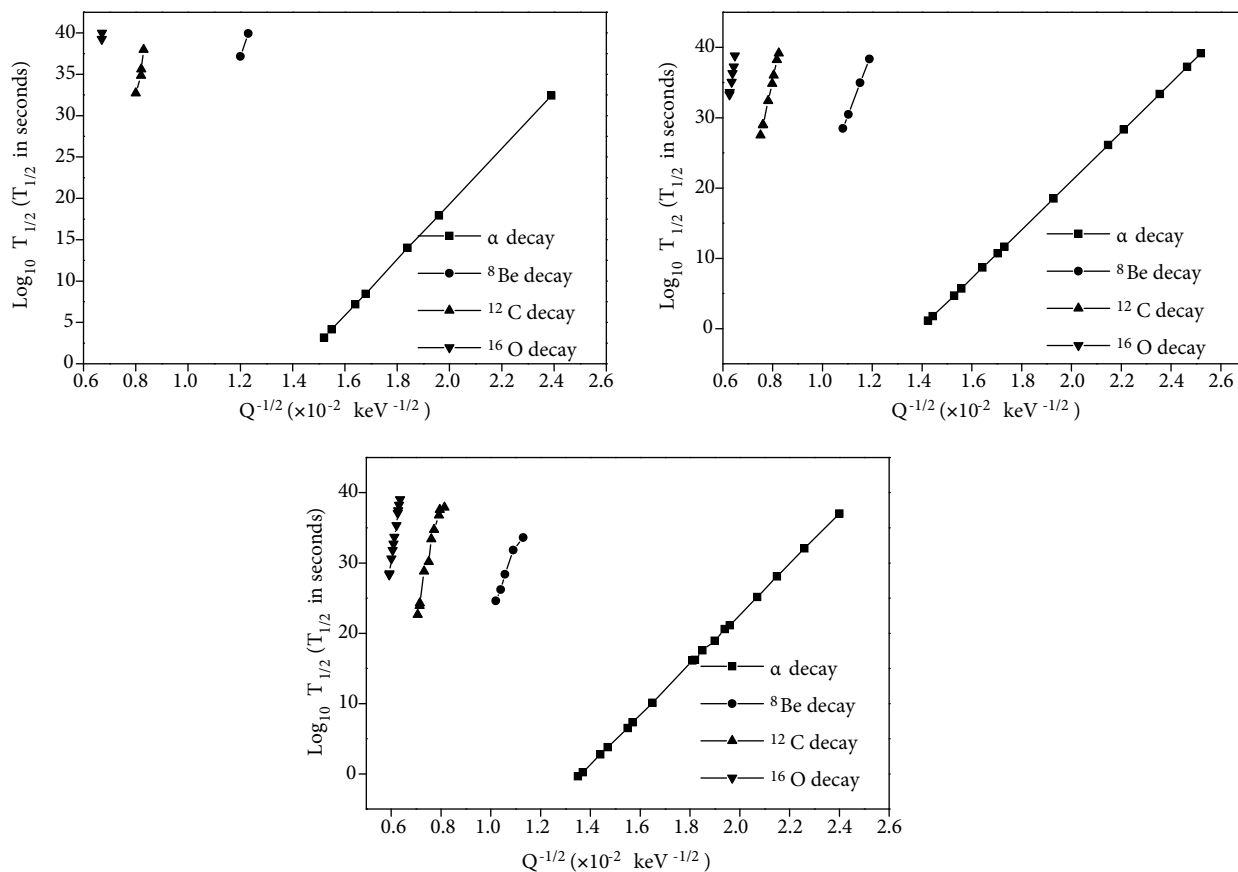


**Figure 5.** Geiger–Nuttall plots of proton-rich Dy (top left), Er (top right), and Yb (bottom) nuclei for different cluster decays.



The predicted half-lives show that neutron-rich Dy, Er, and Yb isotopes could be candidates for cluster radioactivity that are totally different in nature from proton-rich isotopes. The neutron-rich isotopes are found to be stable against  $\alpha$  decay and other  $\alpha$ -like cluster decays, but metastable with respect to emission of highly neutron-rich clusters. Although the most probable light clusters seem to be acutely exotic in nature and the corresponding decays are with extremely short half-lives, the existence of clusters of similar nature has been suggested by Sushil Kumar (e.g.,  ${}_{28}^{78}\text{Ni}$ ) in another study on cluster decays of rare earth nuclei [10] and by Bogdanov et al. (e.g.,  ${}_{1}^5\text{H}$  and  ${}_{2}^6\text{He}$ ) [29]. Still, many of the heavy cluster decays from neutron-rich isotopes are characterized by measurable half-lives. Proton-rich isotopes do not show any Sn radioactivity, while neutron-rich isotopes exhibit the same, which may be understood in terms of daughter shell effects. Although the cluster radioactivity of neutron-rich isotopes of the rare earth nuclei under consideration may not be realized due to the extremely short half-lives, instability of some of the probable light clusters, and lack of measured masses to calculate the Q-value reliably, it is to be pointed out that the theoretical study of the same opens up a possibility for new magic numbers around 66 for proton number and near 86 and 106 for neutron number.

#### 4. Conclusions

Rare earth nuclei provide a fertile region for the study of cluster radioactivity. Even though cluster radioactivity is not experimentally detected in this region, fission model calculations in the 3 nuclei Dy, Er, and Yb in the mass range  $150 < A < 190$  suggest some cluster emissions with half-lives in the measurable range. The agreement between the experimental and predicted half-lives of  $\alpha$  emission in rare earth nuclei and those of cluster decays in the actinide region reiterates the suitability of the model used. All the proton-rich isotopes of Dy, Er, and Yb exhibit the same characteristics with respect to the probable clusters and shell closure property of daughter. Also, these calculations are in good agreement with the previously observed shell effects in cluster radioactivity [6],[14],[15], [16], [30]. The effect of centrifugal potential in half-life is also evident in the study. The neutron-rich counterparts are found to be more feasible for cluster radioactivity, even though some of the most probable light clusters predicted are highly exotic and have extremely short half-lives. A common observation about the neutron-rich isotopes of these nuclei (except  ${}^{174}\text{Dy}$ ) is that the decay rate for the most probable clusters reduces with increasing neutron number, i.e. the neutron excess increases the stability. The same observation was made by Santhosh [31] in the case of radium isotopes. The most striking point observed is the emergence of new magic numbers around 66 for proton number and around 86 and 106 for neutron number.

#### Acknowledgements

One of the authors (KKG) expresses gratitude to UGC, Govt. of India for the grant in aid under the FIP scheme.

#### References

- [1] A. Sandulescu, D. Poenaru and W. Greiner, *Sov. J.Part. Nucl.*, **11**, (1980), 528.
- [2] H. J. Rose and G. A. Jones, *Nature (London)*, **307**, (1984), 245.
- [3] D. N. Poenaru and W. Greiner, Handbook of Nuclear Properties, ed. Dorin N. Poenaru, Walter Greiner, (Oxford University Press, New York, 2008) p. 131.
- [4] G. Royer, R. K. Gupta and V. Yu. Denisov, *Nucl. Phys.*, **A632**, (1998), 275.
- [5] R. Bonetti and A. Guglielmetti, *Romanian reports in Physics*, **59**, (2007), 301.

- [6] S. K. Arun and R. K. Gupta, *Phys. Rev.*, **C80**, (2009), 034317.
- [7] W. Greiner, H.J. Fink, J. A. Maruhn and W. Scheid, *Zeitschrift fuer Physik*, **268**, (1974), 321.
- [8] J. A. Maruhn, W. Greiner and W. Scheid, Theory of fragmentation in heavy ion collisions, ed. R. Bock, vol **II**, (North Holland, Amsterdam, 1980) p.399.
- [9] D. N. Poenaru, W. Greiner and R. Gherghescu, *Phys. Rev.*, **C47**, (1993), 2030.
- [10] S. Kumar, *J. Phys. Conference Series*, **282**, (2011), 012015.
- [11] D. N. Poenaru, R. A. Gherghescu and W. Greiner, *Phys. Rev. Lett.*, **107**, (2011), 062503.
- [12] D. N. Poenaru, R. A. Gherghescu and W. Greiner, *Phys. Rev.*, **C85**, (2012), 034615.
- [13] M. A. Hooshyar, I. Reichstein and F. B. Malik, Nuclear fission and cluster radioactivity—an energy density functional approach, (Springer-Verlag, Berlin, 2005) p. 153.
- [14] H. F. Zhang, J. M. Dong, G. Royer, W. Zuo and J. Q. Li, *Phys. Rev.*, **C80**, (2009), 037307.
- [15] S. S. Malik and R. K. Gupta, *Phys. Rev.*, **C39**, (1989), 1992.
- [16] D. N. Poenaru, M. Ivascu, A. Sandulescu and W. Greiner, *Phys. Rev.*, **C32**, (1985), 572.
- [17] M. Goncalves, S. B. Duarte, F. Garcia and O. Rodriguez, *Comp. Phys. Communications*, **107**, (1997), 246.
- [18] S. B. Duarte, O. A. P. Tavares, F. Guzman and A. Dimarco, *Atomic data and Nuclear data tables*, **80**, (2002), 235.
- [19] G. Audi and A. H. Wapstra, *Nucl. Phys.*, **A595**, (1995), 409.
- [20] S. B. Duarte, O. Rodriguez and O. A. P. Tavares, *Phys. Rev.*, **C57**, (1998), 2516.
- [21] O. Rodriguez, F. Guzman, S. B. Duarte and O. A. P. Tavares, *Phys. Rev.*, **C59**, (1999), 253.
- [22] M. Goncalves and S. B. Duarte, *Phys. Rev.*, **C48**, (1993), 2409.
- [23] S. B. Duarte and M. Goncalves, *Phys. Rev.*, **C53**, (1996), 2309.
- [24] M. Gaudin, *J. Phys. (France)*, **35**, (1974), 885.
- [25] R. K. Gupta, S. Singh, R. K. Puri and W. Scheid, *Phys. Rev.*, **C47**, (1993), 561.
- [26] G. Audi, A. H. Wapsra and C. Thibault, *Nucl. Phys.*, **A729**, (2003), 337.
- [27] D. N. Poenaru, R. A. Gherghescu and W. Greiner, *J. Phys. G: Nucl. Part. Phys.*, **39**, (2012), 015105.
- [28] C. Qi, F. R. Xu, R. J. Liotta and R. Wyss, *Phys. Rev. Lett.*, **103**, (2009), 072501.
- [29] D. D. Bogdanov, M. S. Golovkov, A. M. Rodin, S. I. Sidorchuk, R. S. Slepnev, S. V. Stepantsov, G. M. Ter-Akopian, R. Wolski, V. A. Gorshkov, M. L. Chelnokov, Yu. Ts. Oganessian, A. A. Korshennikov, E. Yu. Nikolskii, I. Tanihata, F. Hanappe, T. Materna, L. Stuttge and A. H. Ninane, *Proceedings of the International Symposium on New Projects and Lines of Research in Nuclear Physics*, Messina, Italy, (2002), 106.
- [30] S. Kumar, D. Bir and R. K. Gupta, *Phys. Rev.*, **C51**, (1995), 1762.
- [31] K. P. Santhosh, *Phys. Scr.*, **81**, (2010), 015203.